BIOORGANIC CHEMISTRY **23,** 193–216 (1995)

Reactions of Cysteine and Cysteinyl Derivatives with Dopamine-*o*-quinone and Further Insights into the Oxidation Chemistry of 5-*S*-Cysteinyldopamine: Potential Relevance to Idiopathic Parkinson's Disease

FA ZHANG[1] AND GLENN DRYHURST[2]

Department of Chemistry and Biochemistry, University of Oklahoma, Norman, Oklahoma 73019

Received March 13, 1995

Recent studies suggest that elevated rates of autoxidation of dopamine (DA) in the cytoplasm of neuromelanin-pigmented dopaminergic cell bodies in the substantia nigra (SN) and/or reactions of its proximate oxidation product, DA-*o*-quinone, with glutathione (GSH) or L-cysteine (CySH) might yield endotoxins that play roles in the pathogenesis of idiopathic Parkinson's Disease (PD). In this study the reactions between DA-*o*-quinone and CySH and some cysteine derivatives have been studied. The reactions between DA-*o*-quinone and CySH or cysteine methyl ester are rapid and give the corresponding 5-*S*-cysteinyl conjugates of DA as the predominant products. By contrast, the reaction between the sterically hindered D-penicillamine methyl ester (PME) and DA-*o*-quinone is much slower to give, initially, a mixture of the 2-*S*-, 5-*S*-, and 6-*S*-PME conjugates of DA. These conjugates are then further oxidized by unreacted DA-*o*-quinone to give a complex mixture of products which include 7-(2-aminoethyl)-5-hydroxy-2,2-dimethyl-1,4-benzothiazine-3-carboxylic acid methyl ester (**13**). Large increases in the 5-*S*-cysteinyldopamine (5-*S*-CyS-DA)/DA concentration ratio have been measured in the Parkinsonian SN and have been interpreted to reflect elevated rates of DA autoxidation in this structure that degenerates in PD. However, the present study reveals that at physiological pH 5-*S*-CyS-DA is not only more easily oxidized than DA but a bicyclic *o*-quinone imine (**5**) intermediate is formed that can chemically oxidize the former conjugate in a reaction that leads to 7-(2-aminoethyl)-3,4-dihydro-5-hydroxy-2*H*-1,4-benzothiazine-3-carboxylic acid (**6**). Compound **6** is lethal when administered into the brains of mice. However, this putative dihydrobenzothiazine endotoxin is even more easily oxidized than 5-*S*-CyS-DA in a rather complex reaction that ultimately forms 7-(2-aminoethyl)-5-hydroxy-1,4-benzothiazine-3-carboxylic acid (**15**). Although this benzothiazine could not be isolated it was identified by comparison of its electrochemical and spectroscopic properties in solution with those of **13**. The results of this study suggest that benzothiazine **15** might serve as a better analytical marker molecule than 5-*S*-CyS-DA for either elevated rates of DA autoxidation and/or for roles of GSH and CySH in the neurodegenerative mechanisms in the SN that contribute to PD.

Parkinson's Disease (PD) is a neurodegenerative brain disorder that results in hypokinesia, rigidity, and tremor. These symptoms are caused in large part by a severe deficiency of the catecholaminergic neurotransmitter dopamine (DA) in the

[1] Current address: Agricultural Research Division, American Cyanamid Company, P.O. Box 400, Princeton, NJ 08543.

[2] To whom correspondence should be addressed.

0045-2068/95 $12.00

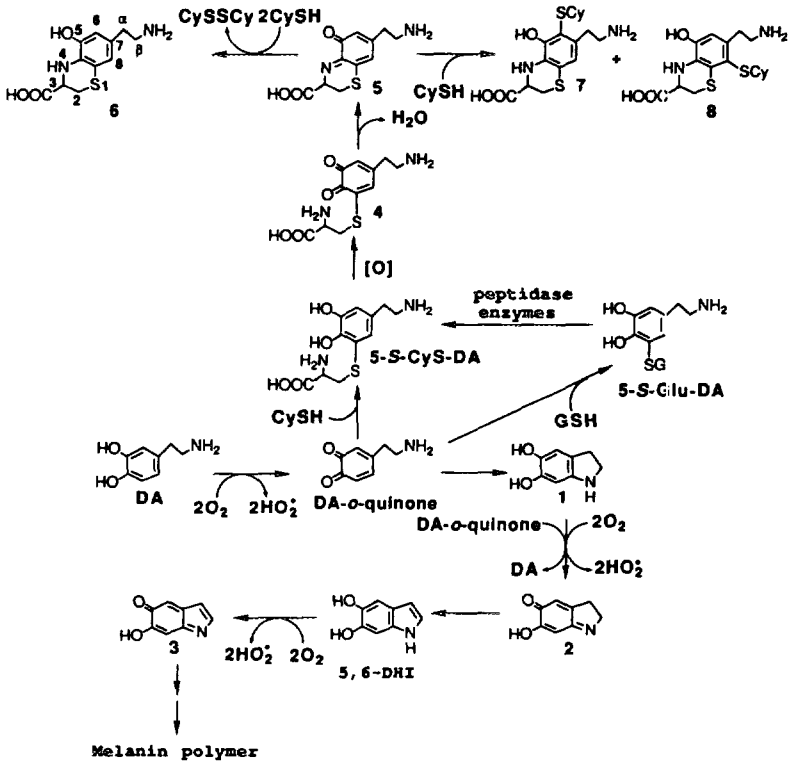

SCHEME I

striatum. This deficiency results from a selective and progressive degeneration of nigrostriatal dopaminergic neurons (*1*) caused by pathological processes that are believed to occur in their cell bodies in the substantia nigra (SN) pars compaca (*2*). Current information suggests that these pathological processes include oxidative stress (*3–5*) and a mitochondrial complex I (NADH CoQ_1 reductase) deficiency (*6, 7*), although the fundamental mechanisms underlying these processes are unknown. Dopaminergic SN cell bodies in the normal human brain are pigmented with black neuromelanin, a polymer formed within the cytoplasm of these neurons as a result of autoxidation of DA (*8, 9*). Chemical degradation of human SN neuromelanin yields products which suggest that this polymer is composed of both indolic residues and residues derived from 5-*S*-cysteinyldopamine (5-*S*-CyS-DA) (*10*). Based upon chemical (*8, 9*) and electrochemical (*11–13*) studies it appears that the indolic residues in neuromelanin result from a pathway where DA is initially autoxidized to DA-*o*-quinone which undergoes an intramolecular cyclization reaction to give 5,6-dihydroxyindoline (**1,** Scheme I). The latter compound is more easily oxidized than DA and is therefore further oxidized by molecular oxygen and/or DA-*o*-quinone (*12, 13*) to *p*-quinone imine **2,** which rearranges to 5,6-dihydroxyindole (5,6-DHI). Further oxidation of 5,6-DHI then gives the indolic *para*-quinone imine

3 that polymerizes to black indolic melanin. Residues derived from 5-*S*-CyS-DA result from the facile nucleophilic addition of L-cysteine (CySH) or glutathione (GSH) to DA-*o*-quinone. In the latter case 5-*S*-qlutathionyldopamine (5-*S*-Glu-DA) is apparently hydrolyzed by intraneuronal peptidase enzymes to 5-*S*-CyS-DA (Scheme I) (*10*). *In vitro* experiments have demonstrated that oxidations of DA in aqueous solutions at physiological pH give black melanin polymer only when the concentrations of CySH or GSH are low relative to that of the neurotransmitter (*10, 14*). Such observations have led Carstam *et al.* (*10*) to conclude that when indolic residues are incorporated into insoluble SN neuromelanin both CySH and GSH must be virtually absent in dopaminergic cell bodies. Histochemical studies have also revealed that there is probably little or no GSH in neuronal cell bodies in any region of the brain and that this tripeptide is largely localized in glia, axons, and nerve terminals (*15, 16*).

Formation of indolic neuromelanin within SN cells implies that these cell bodies must possess a weak antioxidant defense system. Only under such conditions could DA-*o*-quinone escape reduction to DA and cyclize to **1** and 5,6-DHI, the precursors of neuromelanin. In fact, not only GSH (*10, 17, 18*) but also ubiquinols and α-tocopherol levels (*19*) are low in the mammalian SN compared to other brain regions. Furthermore, the mouse SN, for example, has the highest levels of malondialdehyde (an index of lipid peroxidation) of any brain region (20). Such peroxidative damage would result from DA autoxidation in reactions that generate $O_2^- \cdot$ (Scheme I) and thence H_2O_2, which, in the presence of trace levels of transition metal ions (e.g., Fe^{2+}), can produce the highly cytotoxic hydroxyl radical ($HO\cdot$) (*21, 22*). Indeed, such reactions have been suggested (*23, 24*) to contribute to the normal age-dependent degeneration of nigrostriatal dopaminergic neurons (*25*). However, it has been demonstrated that in the SN of PD patients there is a significant decrease in the neuromelanin content of surviving pigmented cells (*26, 27*). Furthermore, the more heavily neuromelanin-pigmented SN neurons appear to be more vulnerable to degeneration in the Parkinsonian brain (*27, 28*). These observations suggest that dopaminergic SN cells having the highest basal levels of DA autoxidation (and hence the heaviest neuromelanin pigmentation) are particularly vulnerable to degeneration in PD and that as the disease progresses the neuromelanin pathway is either blocked or diverted leading to depigmentation. Some potentially important insights into mechanisms that might contribute to this diversion can be drawn from measurements of the levels of 5-*S*-CyS-DA, formed by the reactions shown in Scheme I, in normal, aging, and Parkinsonian brains (*29–31*). For example, the 5-*S*-CyS-DA/DA concentration ratios measured in the striatum and SN of human brain tissue at autopsy have been found to increase with the degree of depigmentation and degeneration of SN cells (*31*). Furthermore, the 5-*S*-CyS-DA/DA ratio in the SN of a patient clinically diagnosed with PD was approximately an order of magnitude greater than that measured in patients without depigmentation and degeneration of the SN (*31*). These observations have been interpreted to indicate an increased rate of DA autoxidation in depigmenting and degenerating SN neurons, an effect that becomes particularly pronounced in the Parkinsonian brain (*31*). An increased rate of DA autoxidation in the SN, which normally contains little or no free GSH or CySH (*10, 15, 16*), would be expected to result in more rapid formation

of indolic neuromelanin polymer and hence increased pigmentation of degenerating SN neurons. However, in the Parkinsonian SN precisely the opposite effects occur, i.e., the more heavily pigmented cells appear to be preferentially vulnerable to degeneration (*27, 28*) and as they degenerate they become progressively depigmented (*26, 27*). It has recently been reported that the activity of only one GSH-related enzyme, γ-glutamyltranspeptidase, is significantly elevated in the Parkinsonian SN (*32*). One function of this enzyme is to translocate extracellular GSH into cells, including neurons, via the γ-glutamylcycle (*33*). Furthermore, in the Parkinsonian brain only the SN is depleted of GSH and this depletion is not accompanied by a corresponding increase in the oxidized form of the tripeptide, i.e., GSSG (*32, 34, 35*). Additionally, levels of GSH in the SN of patients with incidental Lewy body disease, an early presymptomatic stage of PD (*36*), are decreased to the same extent as those in patients with advanced PD without any corresponding increase in GSSG (*34*). Thus, decreased nigral GSH levels appear to be a very early component of the pathological processes that underlie PD. The decrease in nigral GSH levels in PD does not appear to be related to decreased activity of γ-glutamylcysteine synthetase, the rate-limiting enzyme for the biosynthesis of the tripeptide, or to alterations in GSH peroxidase, GSSG reductase, or GSH transferase activities (*32, 37, 38*). Thus, in the Parkinsonian SN, the biochemical systems for GSH biosynthesis and for conversion of GSSG to GSH do not appear to be compromised, suggesting, perhaps, that the tripeptide is being siphoned off by reaction with some exogenous or endogenous species. Based upon these observations we have recently proposed (*14*) that a key step in the pathoetiology of PD might involve the translocation of GSH (or CySH), biosynthsized in glial cells (*39, 40*), into the cytoplasm of neuromelanin-pigmented SN cell bodies. This GSH (or CySH) would be expected to scavenge DA-*o*-quinone, the proximate autoxidation product of DA and precursor of indolic neuromelanin, leading to an increase in the 5-*S*-CyS-DA/DA ratio and diversion of the neuromelanin pathway (*10, 14*), hence accounting for the depigmentation of SN neurons. However, 5-*S*-CyS-DA is significantly more easily oxidized than DA (*14*). Thus, under conditions where cytoplasmic DA is autoxidized in neuromelanin-pigmented SN cell bodies, 5-*S*-CyS-DA would also be expected to be even more readily oxidized. Some insights into the oxidation chemistry of 5-*S*-CyS-DA have been obtained in a recent *in vitro* study in which DA was electrochemically oxidized in the presence of a large (i.e., five-fold) molar excess of CySH at physiological pH. In this reaction DA-*o*-quinone is avidly scavenged by CySH to give 5-*S*-CyS-DA, which is further oxidized to *o*-quinone **4** (Scheme I). The latter *o*-quinone then undergoes a very rapid intramolecular cyclization to the bicyclic *o*-quinone imine **5**, which appears to be a key precursor of many secondary products. Thus, in the presence of a large excess of free CySH, **5** is apparently partially reduced to 7-(2-aminoethyl)-3,4-dihydro-5-hydroxy-2*H*-1,4-benzothiazine-3-carboxylic acid (**6**) or is attacked by CySH to give the 6-*S*- and 8-*S*-cysteinyl conjugates of **6**, i.e., **7** and **8**, respectively (Scheme I). Further facile oxidations of **6–8** in the presence of free CySH ultimately results in the formation of a very large number of products, most of which remain to be identified. Dihydrobenzothiazine **6** and its 6-*S*-(**7**) and 8-*S*-(**8**) cysteinyl conjugates are lethal when administered into the brains of laboratory mice having LD_{50} values of 14, 17, and

70 μg (administered in 5.0 μl of isotonic saline solution), respectively (*14*). These observations suggest that increasing substitutions of CySH residues into **6** decrease the toxicity of this dihydrobenzothiazine. Indeed, the 6,8-bi-*S*-cysteinyl conjugate of **6** is not lethal at doses of 100 μg (*14*). Based on these results we have speculated that **6,** in particular, might be an endotoxin formed as a result of an influx of GSH or CySH into pigmented SN cells that contributes to the degeneration of nigrostriatal dopaminergic neurons leading ultimately to PD (*14*). Because of the very large number (>60) of products formed when DA is oxidized in the presence of large molar excesses of CySH it was difficult to fully elucidate mechanistic pathways. Accordingly, preliminary studies have been carried out in which DA was oxidized in the presence of lower molar excesses of CySH (e.g., equimolar DA and CySH) at physiological pH. These studies revealed that significantly fewer products are formed although dihydrobenzothiazine **6** continued to be formed in the initial stages of the reaction in relatively high yields. This observation was rather surprising in view of the fact that **6** is appreciably more easily oxidized than DA or 5-*S*-CyS-DA (*14*). Subsequently, it was found that oxidation of 5-*S*-CyS-DA in the absence of free CySH also gave **6** as a major initial product along with one other major unidentified compound. Oxidation of 5-*S*-CyS-DA via *o*-quinone **4** would, as demonstrated previously (*14*), give bicyclic *o*-quinone imine **5** (Scheme I) not dihydrobenzothiazine **6.** Formation of **6,** therefore, implies that even in the absence of free CySH there must be an alternative pathway to convert **5** to this lethal dihydrobenzothiazine. Unfortunately, insights into the mechanisms underlying this chemistry were hampered by the fact that the second major product of oxidation of 5-*S*-CyS-DA could not be identified owing to its facile decomposition during the isolation procedures employed. In this communication it will be demonstrated that the reaction of a highly substituted analog of CySH, D-penicillamine methyl ester (PME), with DA-*o*-quinone, the proximate oxidation product of DA, leads to products which, based on a comparison of their spectroscopic and electrochemical properties with those of the previously unidentified product of oxidation of 5-*S*-CyC-DA, permit an unequivocal identification of the latter compound. Furthermore, reaction pathways have been elucidated which explain formation of dihydrobenzothiazine **6** as an initial oxidation product of 5-*S*-CyS-DA at physiological pH.

EXPERIMENTAL

Chemicals

Dopamine hydrochloride (DA.HCl), L-cysteine hydrochloride (CySH.HCl), L-cysteine methyl ester (CME) hydrochloride, and D-penicillamine methyl ester (PME; D-2-amino-3-mercapto-3-methylbutanoic acid, hydrochloride salt) were obtained from Sigma (St. Louis, MO) and were used without additional purification.

Apparatus and Methods

Voltammograms were obtained at a pyrolytic graphite electrode (PGE; Pfizer Minerals, Pigments and Metals Division, Easton, PA) having an approximate surface area of 4 mm^2. A conventional three-electrode voltammetric cell was used with a

platinum wire counter electrode and a saturated calomel reference electrode (SCE). Linear sweep and cyclic voltammograms were obtained using a BAS-100A (Bioanalytical Systems, West Layfeyette, IN) electrochemical analyzer. All voltammograms were corrected for iR drop. The PGE was resurfaced prior to recording each voltammogram as described previously (*41*). Controlled potential electrolyses employed a Princeton Applied Research Corp. (Princeton, NJ) model 173 potentiostat. The working electrode consisted of several plates of pyrolytic graphite having a total surface area of approximately 430 cm^2. A three-compartment cell was used in which the working, counter, and reference electrode compartments were separated by a Nafion membrane (type 117, DuPont Co., Wilmington, DE). The working electrode compartment had a capacity of 80 ml. The counter electrode consisted of several plates of pyrolytic graphite suspended into a solution of the supporting electrolyte. The solution in the working electrode compartment was continuously deoxygenated with a vigorous stream of N_2. All potentials are referred to the SCE at ambient temperature (22 ± 2°C).

^1H NMR spectra were recorded on a Varian XL-300 spectrometer. High and low resolution fast atom bombardment mass spectrometry (FAB-MS) employed a VG Instruments (Manchester, UK) model ZAB-E spectrometer. Thermospray mass spectrometry was performed with a Kratos (Manchester, UK) model MS 25/RFA instrument equipped with a thermospray source. Samples analyzed by thermospray mass spectrometry were collected from a conventional high performance liquid chromatography (HPLC) instrument and then introduced into the mass spectrometer via a Rheodyne (Cotati, CA) model 7125 injector equipped with a 2.0-ml sample loop. The solvent was 0.1 M ammonium acetate in deionized water adjusted to pH 4.1 with acetic acid. A flow rate of 1.0 ml/min was used. The thermospray capillary was maintained at 150°C and the source at 250°C. uv-visible spectra were recorded on a Hewlett-Packard 8452A diode array spectrophotometer.

HPLC employed a Gilson (Middleton, WI) gradient system equipped with model 305 and 306 pumps (25-ml pump heads) and a Holochrome detector set at 254 nm. A Rheodyne model 7125 loop injector was used to introduce samples. Two reversed phase columns were employed; a Spherisorb (Phase Sep, Clwyd, UK) S_{10}, ODS-2, 25 × 2.0-cm column and a Regis (Morton Grove, IL) ODS, 10-μm particle size, 25 × 2.1-cm column. A short guard column (1 × 5-cm) packed with Bakerbond C_{18} (J.T. Baker, Phillipsburg, NJ, 10-μm particle size) was used to protect these preparative HPLC columns. In order to separate the products formed in the reaction systems studied for analytical or preparative purposes, six binary gradient procedures were employed which will be referred to as HPLC methods I–VI. For HPLC method I solvents A and B were employed. Solvent A was prepared by adding 30 ml of concentrated ammonium hydroxide solution (NH_4OH) to 4 liters of deionized water; the pH of the resulting solution was adjusted to 3.0 by addition of concentrated trifluoroacetic acid (TFA). Solvent B was prepared by adding 30 ml of NH_4OH to 2 liters of HPLC grade methanol (MeOH) and 2 liters of deionized water; the pH of this solution was adjusted to 3.0 with TFA. The following gradient was employed; 0–2 min, 100% solvent A; 2–35 min, linear gradient to 100% solvent B; 35–55 min, 100% solvent B. The flow rate was 7 ml/min.

For HPLC method II, solvents C and D were employed. Solvent C was prepared

by adding 30 ml of NH_4OH to 4 liters of deionized water; the pH was then adjusted to 7.0 with TFA. Solvent D was prepared by adding 30 ml of NH_4OH to 1 liter of HPLC grade acetonitrile (MeCN), 1 liter of MeOH, and 2 liters of deionized water; the pH was adjusted to 7.0 with TFA. The following gradient was employed: 0–2 min, 100% solvent C; 2–15 min, linear gradient to 30% solvent D; 15–40 min, linear gradient to 40% solvent D; 40–50 min, linear gradient to 100% solvent D; 50–60 min, 100% solvent D. The flow rate was 7.0 ml/min.

HPLC method III employed solvents A and B and the following gradient: 0–2 min, 100% solvent A; 2–10 min, linear gradient to 60% solvent B; 10–30 min, linear gradient to 100% solvent B; 30–40 min, 100% solvent B. The flow rate was 7 ml/min.

For HPLC methods IV–VI solvents E and F were used. Solvent E was prepared by adding TFA to deionized water until the pH was 3.0. Solvent F was prepared by adding TFA to 5% MeCN in deionized water into the pH was 3.0. The following gradients were used. HPLC method IV: 0–2 min, 100% solvent E; 2–20 min, linear gradient to 10% solvent F; 20–25 min, linear gradient to 100% solvent F; 25–30 min, 100% solvent F. HPLC method V: 0–2 min, 100% solvent E; 2–30 min, linear gradient to 100% solvent F: 30–40 min, 100% solvent F. HPLC method VI: 0–2 min, 100% solvent E; 2–15 min, linear gradient to 40% solvent F; 15–20 min, linear gradient to 100% solvent F; 20–30 min, 100% solvent F. The flow rate for methods IV–VI was 7 ml/min. For HPLC methods I–III the Spherisorb column was used; for methods IV–VI the Regis column was used.

Synthesis of DA-o-Quinone

DA.HCl (30 mg; 2.0 mM) was dissolved in 80 ml of 0.1 M HCl and electro-oxidized at pyrolytic graphite electrodes for 30–50 min at 1.0 V. The reaction solution turned from colorless to bright yellow, characteristic of DA-*o*-quinone. HPLC analysis (method I) revealed that during the latter period of reaction DA was converted (≥80%) to DA-*o*-quinone and no other significant products were formed. The uv-visible spectrum, thermospray mass spectrum, and cyclic voltammetry of DA-*o*-quinone were all in agreement with those reported previously (*11*).

Reactions of DA-o-Quinone with Cysteine, Cysteine Methyl Ester (CME), and D-*Penicillamine Methyl Ester (PME)*

CySH.HCl (160 mg), or CME hydrochloride (180 mg), or PME hydrochloride (200 mg) was added to 80 ml of DA-*o*-quinone (ca. 2 mM) in 0.1 M HCl elecrochemically synthesized as described in the preceding paragraph. The reactions were carried out with N_2 gas bubbling vigorously through the solution. Upon addition of CySH or CME the reaction solution changed immediately from bright yellow to a very pale yellow color. Chromatography (HPLC method I) revealed that the major product of reaction of DA-*o*-quinone with CySH (i.e., 5-*S*-CyS-DA) had a retention time (t_R) of 24.8 min. The product formed between DA-*o*-quinone and CME (i.e., **9**) eluted at t_R = 27.2 min. The solutions eluted under these peaks were collected and freeze-dried. The resulting solids were dissolved in the minimum volume of deionized water and the solutions desalted and purified using HPLC method IV. 5-*S*-CyS-DA eluted at t_R = 10.0 min; **9** eluted at t_R = 14.0 min. The solutions

containing desalted and purified 5-*S*-CyS-DA and **9** were freeze-dried. The spectroscopic properties of 5-*S*-CyS-DA (^{1}H NMR, FAB-MS, uv) have been reported previously (*11, 14*).

Addition of PME.HCl to DA-*o*-quinone caused the initially bright yellow solution to turn to a dull yellow color over the course of 20–30 min. HPLC analysis (method I) at the end of this time showed five major chromatographic peaks of products having t_R values of 36.5, 40.5, 44, 50, and 56.5 min, in addition to a large peak of DA and several peaks corresponding to minor, unidentified products. The compounds eluted under the major chromatographic peaks were collected individually. These solutions were then desalted and purified using either HPLC methods VI (compound **10,** t_R = 17 min) or method **V** (**11,** t_R = 24 min; **12,** t_R = 23 min; **13,** t_R = 26 min; **14,** t_R = 23 min). The desalted eluents containing these compounds were then shell frozen and freeze-dried.

Oxidation of 5-S-CyS-DA

5-*S*-CyS-DA (22 mg; 1.0 mM) was dissolved in 80 ml of pH 7.4 phosphate buffer (μ = 0.2) and electrolyzed at 66 mV for 20 min. HPLC analysis (method II) indicated that two major products were formed (**6,** t_R = 22 min; **15,** t_R = 25 min). For preparative purposes the entire volume of the reaction solution (80 ml) was pumped onto the HPLC column and separated using method II. Compound **6** and unreacted 5-*S*-CyS-DA coeluted and were collected together; the eluent containing **15** was also collected. These solutions were further separated, purified, and desalted using HPLC method IV (5-*S*-CyS-DA, t_R = 10 min; **6,** t_R = 30 min; **15,** t_R = 22 min). The purified and desalted solutions were then freeze-dried. Compound **15** decomposed during the freeze-drying process to give a complex mixture of products which remain to be identified. Dihydrobenzothiazine **6** was initially isolated as a pale yellow solid although even when stored in a vacuum dessicator it gradually darkened and ultimately became black. The spectroscopic and chromatographic properties and cyclic voltammetry of **6** were identical to those reported previously for 7-(2-aminoethyl)-3,4-dihydro-5-hydroxy-2*H*-1,4-benzothiazine-3-carboxylic acid (*14*).

Oxidation of 5-S-Cysteinyldopamine Methyl Ester (**9**)

Compound **9** (11.4 mg; 0.5 mM) was dissolved in 80 ml of pH 7.4 phosphate buffer (μ = 0.2) and electro-oxidized at 16 mV for 30 min. HPLC (method I) indicated that two products were formed (**16,** t_R = 31.5 min; **17,** t_R = 35.5 min). For preparative purposes the total volume of the reaction solution was introduced onto the HPLC column and products separated using method III. The eluent solutions containing **16** and **17** were collected and then desalted and purified using HPLC method V. The solutions containing **16** and **17** were freeze-dried. During this process **17** decomposed to several secondary products that remain to be identified.

5-S-Cysteinyldopamine Methyl Ester (**9**)

Compound **9** was isolated as a white solid. In pH 7.4 phosphate buffer (μ = 1.0) **9** exibited a uv spectrum with bands at λ_{max}, nm (log ε_{max}, M^{-1} cm^{-1}) 294 (3.08), 255 sh(3.23), 230 (3.52). FAB-MS (3-nitrobenzyl alcohol matrix) gave m/e = 287.1075

(MH^+, 100%, $C_{12}H_{19}N_2O_4S$; calcd m/e = 287.1066). ^1H NMR (D_2O) gave δ 6.94 (d, $J_{2,6}$ = 2.1 Hz, 1H, C(6)-H), 6.84 (d, $J_{2,6}$ = 2.1 Hz, 1H, C(2)-H), 4.34 (t, J = 4.8 Hz, 1H, C(b)-H), 3.70 (dd, J = 15.6 Hz, J = 4.8 Hz, 1H, C(a)-H), 3.32. (dd, J = 15.6 Hz, J = 4.8 Hz, 1H, C(a)-H), 3.19 (t, J = 7.3 Hz, 2H, C (β)-H_2), 2.84 (t, J = 7.3 Hz, 2H, C(α)-H_2). 2D-correlated spectroscopy (COSY) experiments revealed that the following reasonances were coupled: 6.94 and 6.84; 4.34 and 3.70; 4.23 and 3.32; 3.70 and 3.32; 3.19 and 2.84.

N-[4-(2-Aminoethyl)-2-[(2-amino-3-methoxy-1,1-dimethyl-3-oxopropyl)thio]-6-hydroxyphenyl]-3-mercapto-valine Methyl Ester (**10**)

Compound **10** was isolated as a very pale yellow solid. In pH 7.4 phosphate buffer **10** exhibited uv bands at λ_{max} 320(sh), 302, and 216 nm. FAB-MS (3-nitrobenzyl alcohol matrix) gave m/e = 458.1787 [(M-2H) H^+, 10%, $C_{20}H_{32}N_3O_5S_2$; calcd m/e = 458.1783]. ^1H NMR (D_2O) gave δ 7.03 (d, $J_{3,5}$ = 2.1 Hz, 1H, C(3)-H), 6.99 (d, $J_{3,5}$ = 2.1 Hz, 1H, C(5)-H), 4.18 (s, 1H, C(b)-H), 3.90 (s, 1H, C(b′)-H), 3.90 (s, 3H, CO_2CH_3), 3.81 (s, 3H, CO_2CH_3), 3.24 (t, J = 7.5 Hz, 2H, C(β)-H2), 2.90 (t, J = 7.5 Hz, 2H, C(α)-H_2), 1.55 (s, 3H, C(a)-CH_3), 1.54 (s, 3H, C(a)-CH_3), 1.43 (s, 3H, C(a′)-CH_3), 1.41 (s, 3H, C(a′)-CH_3). Cyclic voltammetry of **10** in pH 7.4 phosphate buffer at a sweep rate (ν) of 100 mVs^{-1} showed three oxidation peaks having peak potentials (E_p) at 28, 132, and 608 mV on the initial anodic sweep. After sweep reversal, small indistinct reduction peaks were observed at ca. 100 and −48 mV. At ν = 10 Vs^{-1} the first two oxidation peaks merged to give one peak at E_p = 147 mV; after scan reversal a reversible reduction peak, E_p = 99 mV, appeared having the same peak current (i_p) as the initial oxidation peak.

8-(2-Aminoethyl)-3,7-dihydro-5-hydroxy-2,2-dimethyl-7-oxo-2H-1,4-benzothiazine-3-carboxylic Acid Methyl Ester (**11**)

Compound **11** was isolated as a blue solid. In pH 7.4 phosphate buffer **11** exhibited uv-visible bands at λ_{max} 572, 314(sh), 260, and 226 nm. FAB-MS (3-nitrobenzyl alcohol matrix) gave m/e = 311.1059 (MH^+, 100%, $C_{14}H_{19}N_2O_4S$; calcd m/e = 311.1066). ^1H NMR (D_2O) gave δ 6.58 (s, 1H, C(6)-H), 4.28 (s, 1H, C(3)-H), 3.78 (s, 3H, CO_2CH_3), 3.21 (t, J = 7.2 Hz, 2H, C(β)-H_2), 2.81 (t, J = 7.2 Hz, 2H, C(α)-H_2), 1.44 (s, 3H, C(2)-CH_3), 1.37 (s, 3H, C(2)-CH_3). Cyclic voltammograms (ν = 100 mVs^{-1}) of **11** in pH 7.4 phosphate buffer exhibited a reduction peak at E_p = −262 mV on the initial cathodic sweep and, following scan reversal, a reversible oxidation peak of equal height at E_p = −244 mV.

7-(2-Aminoethyl)-6-[(2-amino-3-methoxy-1,1-dimethyl-3-oxopropyl)thio]-3,4-dihydro-5-hydroxy-2,2-dimethyl-2H-1,4-benzothiazine-3-carboxylic Acid Methyl Ester(**12**)

Compound **12** was isolated as a yellow solid. In pH 7.4 phosphate buffer **12** exhibited uv bands at λ_{max} 324 and 244 nm. FAB-MS (3-nitrobenzyl alcohol matrix) gave m/e = 458.1769 (MH^+, 93%, $C_{20}H_{32}N_3O_5S_2$; calcd m/e 458.1783). ^1H NMR (D_2O) gave δ 6.78 (s, 1H, C(8)-H), 4.42 (s, 1H, C(3)-H), 4.14 (s, 1H, C(b)-H), 3.83

(s, 3H, CO_2CH_3), 3.73 (s, 3H, CO_2CH_3), 3.3–2.8 (m, 4H, C(α)-H_2 and C(β)-H_2), 1.48–1.46 (m, 12H, 2 × C(2)-CH_3 and 2 × C(a)-CH_3). Cyclic voltammetry (ν = 100 mVs^{-1}) of **12** in pH 7.4 phosphate buffer showed an oxidation peak at E_p = 130 mV followed by a shoulder at E_p = 200 mV and a further broad oxidation peak at $E_p \approx 590$ mV on the initial anodic sweep. After scan reversal a small, broad reduction peak appeared at E_p = 120 mV.

7-(2-Aminoethyl)-5-hydroxy-2,2-dimethyl-1,4-benzothiazine-3-carboxylic Acid Methyl Ester (**13**)

Compound **13** was isolated as a yellow solid. In pH 7.4 phosphate buffer **13** exhibited uv bands at λ_{max} 340, ca. 300 sh, 242 and 230 nm. FAB-MS (3-nitrobenzyl alcohol matrix) gave m/e = 295.1115 (MH^+, 100%, $C_{14}H_{19}N_2O_3S$; calcd m/e = 295.116). ^1H NMR (D_2O) gave δ 6.82 (d, $J_{6,8}$ = 2.0 Hz, 1H, C(8)-H), 6.75 (d, $J_{6,8}$ = 2.0 Hz, 1H, C(6)-H), 3.93 (s, 3H, CO_2CH_3), 3.24 (t, J = 7.28 Hz, 2H, C(β)-H_2), 2.91 (t, J = 7.28 Hz, 2H, C(α)-H_2), 1.50 (s, 6H, 2 × C(2)-CH_3). Cyclic voltammetry (ν = 100 mVs^{-1}) of **13** in pH 7.4 phosphate buffer exhibited a single, irreversible oxidation peak at E_p = 612 mV on the initial anodic sweep.

8-[(1,1-Dimethyl-2-amino-2-carboxyethyl methyl ester)thio]-7-(2-aminoethyl)-5-hydroxy-2,2-dimethyl-1,4-benzothiazine-3-carboxylic Acid Methyl Ester (**14**)

Compound **14** was isolated as a yellow solid. In pH 7.4 phosphate buffer **14** exhibited uv bands at λ_{max} 354, 232, and 216 nm. FAB-MS (3-nitrobenzyl alcohol matrix) gave m/e = 456.1617 (MH^+, 100%, $C_{20}H_{30}N_3O_5S_2$; calcd m/e = 456.1627). ^1H NMR (D_2O) gave δ 7.06 (s, 1H, C(6)-H), 4.11 (s, 1H, C(b)-H), 3.97 (s, 3H, CO_2CH_3), 3.84 (s, 3H, CO_2CH_3), 3.65–3.06 (m, 4H, C(α)-H_2 and C(β)-H_2), 1.57 (s, 6H, 2 × CH_3), 1.44 (s, 3H, CH_3), 1.40 (s, 3H, CH_3). Cyclic voltammetry (ν = 100 mVs^{-1}) of **14** in pH 7.4 phosphate buffer exhibited two overlapping irreversible oxidation peaks (E_p = 590 and 680 mV) on the initial anodic sweep.

7-(2-Aminoethyl)-3,4-dihydro-5-hydroxy-2H-1,4-benzothiazine-3-carboxylic Acid Methyl Ester (**16**)

Compound **16** was obtained as a very pale yellow solid. In pH 7.4 phosphate buffer **16** exhibited uv bands at λ_{max} 304 and 234 nm. FAB-MS (3-nitrobenzyl alcohol matrix) gave m/e = 269.0974 (MH^+, 100%, $C_{12}H_{17}N_2O_3S$; calcd m/e = 269.0960). ^1H NMR (D_2O) gave δ 6.56 (d, $J_{6,8}$ = 1.8 Hz, 1H, C(8)-H), 6.54 (d, $J_{6,8}$ = 1.8 Hz, 1H, C(6)-H), 4.63 (t, J = 4.2 Hz, 1H, C(3)-H), 3.74 (s, 3H, CO_2CH_3), 3.34 (dd, J = 13.2 Hz, J = 4.2 Hz, 1H, C(2)-H), 3.27 (dd, J = 13.2 Hz, J = 4.2 Hz, 1H, C(2)-H), 3.16 (t, J = 14.1 Hz, 2H, C(β)-H_2), 2.77 (t, J = 14.1 Hz, 2H, C(α)-H_2).

RESULTS

Reactions of CySH, CME, and D-*PME with DA-o-Quinone*

DA-*o*-quinone is the proximate product of the electrochemical oxidation of DA over a wide range of pH (*11*). However, at physiological pH DA-*o*-quinone is unstable and rapidly cyclizes to 5,6-dihydroxyindoline (**1**) the precursor of black

indolic melanin polymer (Scheme I) (*11–13*). Thus, in order to study the direct interactions between DA-*o*-quinone and CySH, CME, and PME, it ws necessary to oxidize DA in solution at low pH (0.1 M HCl), conditions under which the quinone is relatively stable (*11*). HPLC (method I) of a solution of DA (2.0 mM) in 0.1 M HCl both before and after controlled potential electro-oxidation (1.0 V; 30 min) revealed that the neurotransmitter was almost quantitatively transformed into DA-*o*-quinone. The latter compound was identified on the basis of its characteristic uv-visible spectrum, thermospray mass spectrum, and cyclic voltammetry as described previously (*11*).

Addition of a sixfold molar excess of CySH to a thoroughly deoxygenated solution of DA-*o*-quinone (ca. 2 mM) in 0.1 M HCl resulted in the initially bright yellow solution becoming almost colorless. HPLC (method I) of the product solution revealed that the chromatographic peak of DA-*o*-quinone had disappeared and that one major peak was present. The compound responsible for this peak was isolated and structurally identified as 5-*S*-CyS-DA. Reaction of CME with DA-*o*-quinone under the same experimental conditions also gave one major product identified as 5-*S*-CyS-DA methyl ester (**9**). A number of minor products were also formed as a result of the reactions between DA-*o*-quinone and CySH and CME although these were not isolated and identified.

The reaction between DA-*o*-quinone (ca. 2 mM) and a sixfold molar excess of PME in 0.1 M HCl was considerably slower than that observed with CySH or CME and required, based upon spectroscopic measurements and HPLC analysis (method I), about 20–30 min to reach completion (i.e., complete removal of DA-*o*-quinone). At the end of this time HPLC of the resulting solution revealed the presence of more than nine products in addition to a significant peak for DA. The five major reaction products were isolated and spectroscopically identified as *N*-[4-(2-aminoethyl)-2-[(2-amino-3-methoxy-1,1-dimethyl-3-oxopropyl)thio]-6-hydroxyphenyl]-3-mercapto-valine methyl ester (**10**), 8-(2-aminoethyl)-3,7-dihydro-5-hydroxy-2,2-dimethyl-7-oxo-2*H*-1,4-benzothiazine-3-carboxylic acid methyl ester (**11**), 7-(2-aminoethyl)-6-[2-amino-3-methoxy-1,1-dimethyl-3-oxopropyl)thio]-3,4-dihydro-5-hydroxy-2,2-dimethyl-2*H*-1,4-benzothiazine-3-carboxylic acid methyl ester (**12**), 7-(2-aminoethyl)-5-hydroxy-2,2-dimethyl-1,4-benzothiazine-3-carboxylic acid methyl ester (**13**), and 8-[(1,1-dimethyl-2-amino-2-carboxyethyl methyl ester)thiol]-7-(2-aminoethyl)-5-hydroxy-2,2-dimethyl-1,4-benzothiazine-3-carboxylic acid methyl ester (**14**) (see Experimental).

Oxidation of 5-S-CyS-DA and 5-S-CyS-DA Methyl Ester (**9**)

At a slow sweep rate (v = 10 mVs^{-1}) the primary voltammetric oxidation peak of 5-*S*-CyS-DA (1.0 mM) in pH 7.4 phosphate buffer had a peak potential (E_p) of 69 mV. Following controlled potential electro-oxidation of 5-*S*-Cys-DA (1.0 mM; pH 7.4 phosphate buffer) at 66 mV for 20 min HPLC analysis (method II) showed formation of two major products. The compound eluting at t_r = 22 min was isolated and spectroscopically identified (^{1}H NMR, FAB-MS, uv spectra) as 7-(2-aminoethyl)-3,4-dihydro-5-hydroxy-2*H*-1,4-benzothiazine-3-carboxylic acid (**6**) (see *Experimental*). The second major product of this reaction (**15**; t_R = 25 min; method

II) was relatively stable in buffered solution at pH 7.4 and in the HPLC mobile phase (pH 7.0). However, attempts to isolate this compound were unsuccessful owing to its facile transformation into a mixture of unidentified secondary products during the final freeze-drying step. With longer electrolysis times the chromatographic peak of dihydrobenzothiazine **6** decreased and ultimately disappeared. Correspondingly, the peak of **15** increased.

The primary voltammetric oxidation peak of **9** (0.5 mM; 10 mVs^{-1}) at pH 7.4 occurs at E_p = 16 mV. HPLC (method I) of the solution formed following controlled potential electro-oxidation of **9** (1.0 mM) at 16 mV for 20 min in pH 7.4 phosphate buffer revealed that two major products were formed having t_R values of 31.5 and 35.5 min. The product eluting at t_R = 31.5 min was isolated and spectroscopically identified as 7-(2-aminoethyl)-3,4-dihydro-5-hydroxy-2*H*-1,4-benzothiazine-3-carboxylic acid methyl ester (**16**). The second major product (**17**) could not be isolated owing to its decomposition to several unidentified products during the final freeze-drying step. When **9** was electrolyzed for times greater than 20 min, HPLC analysis showed that the chromatographic peak for **16** decreased and disappeared and that for **17** correspondingly increased.

The structures of **15** and **17**, the major ultimate products of controlled potential electro-oxidation of 5-*S*-CyS-DA and **9**, respectively, were assigned by comparisons of their uv spectra, thermospray mass spectra, and voltammetric behaviors with those of 7-(2-aminoethyl)-5-hydroxy-2,2-dimethyl-1,4-benzothiazine-3-carboxylic acid methyl ester (**13**), a stable product of the reaction between DA-*o*-quinone and PME in 0.1 M HCl. Thus, the thermospray mass spectra of **15**, **17**, and **13** exhibited intense pseudomolecular ions (MH^+) at m/e = 253 (100%), 267 (100%), and 295 (100%), respectively. The uv spectra of **15** (λ_{max} = 344, ca. 300 sh, 246 nm), **17** (λ_{max} = 360, ca. 300 sh, 244 nm), and **13** (λ_{max} = 340, ca. 300 sh, 242 nm) at pH 7.4 were also very similar. Voltammograms of **15**, **17**, and **13** (ν = 100 mVs^{-1}) at pH 7.4 exhibited single irreversible oxidation peaks at E_p = 612, 582, and 612 mV, respectively. Based upon such comparisons it was concluded that **15** is 7-(2-aminoethyl)-5-hydroxy-1,4-benzothiazine-3-carboxylic acid and **17** its methyl ester. Furthermore, controlled potential electro-oxidations of **6** (66 mV) or **16** (16 mV) in pH 7.4 phosphate buffer resulted in formation of benzothiazines **15** or **17**, respectively, as the major reaction products along with additional minor unidentified compounds.

REACTION PATHWAYS

In strongly acidic solution (e.g., 0.1 M HCl) the exocyclic amino group of DA-*o*-quinone is fully protonated such that its intramolecular cyclization to 5,6-dihydroxyindoline (**1**) is effectively blocked (*11–13*). Thus, under such acidic conditions reactions between DA-*o*-quinone and CySH, CME, and PME can be studied directly. The reaction between CySH and CME with DA-*o*-quinone at low pH is rapid and results in the formation of 5-*S*-CyS-DA and **9**, respectively (Scheme II). Additional minor products are formed in these reactions but only in low yields and hence no attempts were made to identify these compounds. The particular

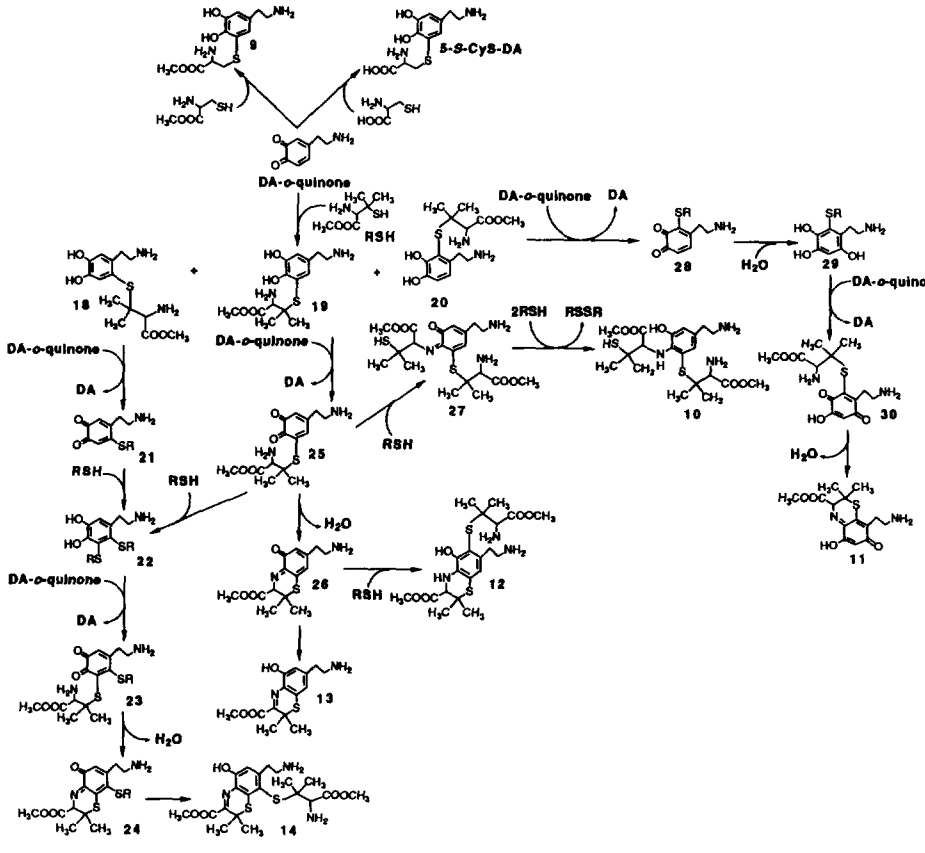

SCHEME II

susceptibility of the C(5)-position of DA-*o*-quinone toward nucleophilic substitution by the sulfhydryl residues of CySH and CME is consistent with the report that the *o*-quinone formed by oxidation of 3,4-dihydroxyphenylalanine (DOPA) reacts with CySH to give 5-*S*-cysteinyl-DOPA (5-*S*-CyS-DOPA) as the predominant product (42).

The reaction between DA-*o*-quinone and PME at low pH is appreciably slower than that with CySH and CME. Furthermore, this reaction leads to the formation of five major products and several unidentified minor products in addition to DA. None of the major products were simple PME conjugates of DA. Nevertheless, the structures of these products (**10–14**, Scheme II) suggest that DA-*o*-quinone is initially attacked by PME to give the 6-*S*-(**18**), 5-*S*-(**19**), and 2-*S*-(**20**) PME conjugates of DA. It is probable that the steric effects of the 2,2-methyl residues of PME account for both its relatively slow reaction with DA-*o*-quinone and its apparent nucleophilic substitution at the C(2)-, C(6)-, and C(5)-positions. The fast reaction between CySH and CME with DA-*o*-quinone rapidly depletes the solution of the

latter compound. By contrast, the rather slow reaction between PME and DA-*o*-quinone results in the initial formation of putative conjugates **18–20** in the presence of significant concentrations of the unreacted quinone. Furthermore, in order to account for formation of **10–14** it is clear that additional oxidation chemistry of **18–20** must occur. Because these reactions were carried out in the absence of molecular oxygen the only available oxidant in solution is DA-*o*-quinone. Cyclic voltammograms (200 mVs^{-1}) of DA (1.0 mM) in 0.1 M HCl show an oxidation peak at E_p = 518 mV and, after scan reversal, a reduction peak of equal peak current at E_p = 490 mV, i.e., $E^{\circ\prime}$ for the DA/DA-*o*-quinone couple in 0.1 M HCl is 504 mV vs SCE. These results indicate that DA-*o*-quinone is a rather strong oxidizing agent under these solution conditions. Because putative conjugates **18–20** have not been isolated it is not possible to measure their oxidation potentials. However, the E_p values (ν = 10 mVs^{-1}) for the primary voltammetric oxidation peaks for 5-*S*-CyS-DA and **9** in 0.1 M HCl are 69 and 16 mV, respectively, i.e., less positive values than $E^{\circ\prime}$ for the DA/DA-*o*-quinone couple. Accordingly, it appears reasonable to conclude that DA-*o*-quinone is responsible for the chemical oxidations of **18–20**. The probable consequences of such oxidations are summarized in Scheme II. Thus, oxidation of **18** by DA-*o*-quinone would yield *o*-quinone **21** (and DA) which, following nucleophilic addition of PME, would yield the 5,6-bi-*S*-PME conjugate of DA, **22**. A second oxidation of **22** by DA-*o*-quinone would then yield *o*-quinone **23** that cyclizes to *o*-quinone imine **24**. Rearrangement (tautomerization) of **24** to its more stable phenolic form would then result in benzothiazine **14**. Oxidation of the putative 5-*S*-PEM conjugate of DA **19** by DA-*o*-quinone would give *o*-quinone **25**. Nucleophilic addition of PME to **25** would yield **22** and, hence, benzothiazine **14**. Alternatively, intramolecular cyclization of **25** would give *o*-quinone imine **26** which rearranges to benzothiazine **13**. Nucleophilic addition of PEM to **26** would account for formation of dihydrobenzothiazine **12**. In order to account for formation of **10**, it is proposed that the amino group of PEM condenses with a carbonyl residue of *o*-quinone **25** to form the Schiff base **27** which is then reduced by free PME. Oxidation of the 2-*S*-PME conjugate of DA (**20**) by DA-*o*-quinone would yield *o*-quinone **28**. Nucleophilic addition of water would then yield the 2-*S*-PME conjugate of 6-hydroxydopamine (6-OHDA), i.e., **29**. A similar reaction has also been reported between DA-*o*-quinone and water at low pH to give 6-OHDA (*43*). Further facile oxidation of **29** by DA-*o*-quinone or, perhaps other putative quinone or quinone imine intermediates of the type shown in Scheme II, would yield *o*-quinone **30** which upon intramolecular cyclization gives **11**.

There are, in principal, many additional reaction pathways that might also contribute to the formation of **10–14** when PME is incubated with DA-*o*-quinone. Nevertheless, formation of significant amounts of DA in these reactions tends to provide support for several key oxidation steps driven by DA-*o*-quinone.

At pH 7.4 both dihydrobenzothiazine **6** and benzothiazine **15** are formed in the early stages of the controlled potential electro-oxidation of 5-*S*-CyS-DA. Because 5-*S*-CyS-DA is initially oxidized to *o*-quinone **4**, which rapidly cyclizes to *o*-quinone imine **5** (Scheme I) (*14*), it becomes clear that a chemical pathway must exist by which **5** is reduced to **6**. Insights into this pathway can be obtained by first considering the redox chemistry of dihydrobenzothiazine **6**. A cyclic voltammogram of **6** (1.0

mM; $\nu = 100$ mVs^{-1}) in pH 7.4 phosphate buffer is shown in Fig. 1A. On the initial anodic sweep the primary oxidation peak $6I_a$ appears ($E_p = 82$ mV), followed by a smaller oxidation peak II_a ($E_p = 145$ mV). At considerably more positive potentials oxidation peak III_a ($E_p = 590$ mV) appears. Following scan reversal, reduction peak II_c forms a reversible couple with oxidation peak II_a. Peak III_a corresponds to the oxidation of benzothiazine **15** (Fig. 1B), the ultimate oxidation product of **6**. The former compound could not be isolated but was identified by comparison of its cyclic voltammetric behavior (Fig. 1B) and spectroscopic properties with that of its 2,2-dimethyl methyl ester analog **13** (Fig. 1C). Insights into the electrochemical and chemical reactions associated with peaks $6I_a$, II_a, and II_c were obtained from cyclic voltammograms of **6** at different sweep rates. At a very slow sweep rate ($\nu = 10$ mVs^{-1}, Fig. 2A) oxidation peak $6I_a$ ($E_p = 53$ mV) is followed by oxidation peak II_a ($E_p = 140$ mV), the peak current (i_p) for peak II_a being approximately one-third that for peak $6I_a$. After scan reversal reduction peak II_c forms a reversible couple with oxidation peak II_a. At $\nu = 100$ mVs^{-1} (Fig. 2B) i_p for peak II_a decreases relative to that for peak $6I_a$, but i_p for peak II_c increases. At υ between 500 mVs^{-1} (Fig. 2C) and 1 Vs^{-1} (Fig. 2D) oxidation peak II_a is not discernable although on the reverse sweep reduction peak II_c ($E_p = 122 \pm 4$ mV) can be observed. With further increases in ν (e.g., 5 Vs^{-1} and 10 Vs^{-1}, Fig. 2E and Fig. 2F, respectively) the peak potential for the reduction peak formed after scan reversal shifts toward more negative potentials ($E_p = 103$ mV at 5 Vs^{-1} and 96 mV at 10 Vs^{-1}). There are several important conclusions that can be drawn from the cyclic voltammograms of **6** presented in Fig. 2. First, at slow sweep rates ($\nu = 10 - 100$ mVs^{-1}) a product is formed in the peak I_a electro-oxidation of **6** that can be oxidized in the peak II_a reaction. Furthermore, the proximate product of the peak II_a oxidation reaction can be reversibly reduced at peak II_c. However, with increasing sweep rates i_p for peak II_a decreases ($\nu = 100$ mVs^{-1}; Fig. 2B) and disappears ($\nu \geq 500$ mVs^{-1}; Fig. 2C–F). Nevertheless, even though peak II_a is not observed at intermediate sweep rates (500 mVs^{-1} – 1 Vs^{-1}) reduction peak II_c continues to be observed (Figs. 2C and 2D). This observation implies that the compound responsible for reduction peak II_c can be formed as a result of both the peak $6I_a$ ($\nu = 500$ mVs^{-1} – 1 Vs^{-1}) and peak II_a (10–100 mVs^{-1}) oxidation reactions. At $\nu \geq 5$ Vs^{-1}, the negative shift of E_p for the reduction peak formed after scan reversal indicates that the peak I_a oxidation product responsible for this peak ($6I_c$) is no longer the same as that which gives rise to peak II_c. Indeed, at such fast sweep rates peak $6I_c$ clearly corresponds to the reversible reduction of the proximate product of the peak $6I_a$ reaction. Recalling that the ultimate product of the controlled potential electro-oxidation of **6** is benzothiazine **15**, plausible reaction pathways that might provide a rationalization of the cyclic voltammetric behaviors shown in Fig. 2 are summarized in Scheme III. Thus, it is proposed that peak $6I_a$ corresponds to the one-electron oxidation of **6** to cation radical **31** that subsequently undergoes two parallel reactions. The first involves a relatively slow deprotonation to give neutral radical **32** which is then oxidized ($1e$) in the peak II_a reaction to *o*-quinone imine **5**. The latter compound is then reduced to **32** in the peak II_c reaction. The relatively small i_p for oxidation peak II_a compared to that for peak I_a even at slow sweep rates (Figs. 2A and 2B) indicates that formation of radical **32** is a relatively minor

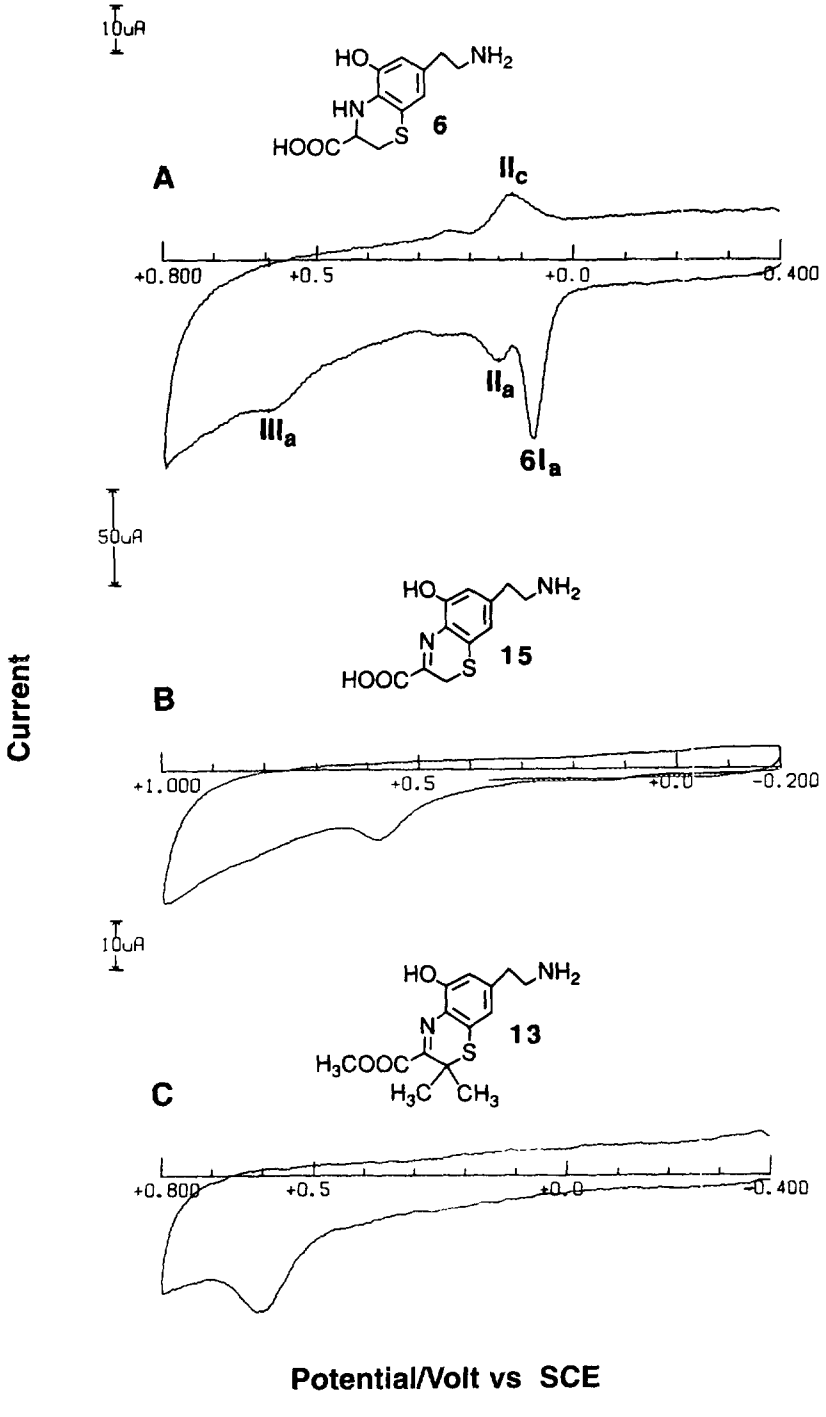

FIG. 1. Cyclic voltammograms at the PGE of (A) dihydrobenzothiazine **6** (1.0 mM), (B) benzothiazine **15**, and (C) benzothiazine **13** in pH 7.4 phosphate buffer. Sweep rate, 100 mVs^{-1}.

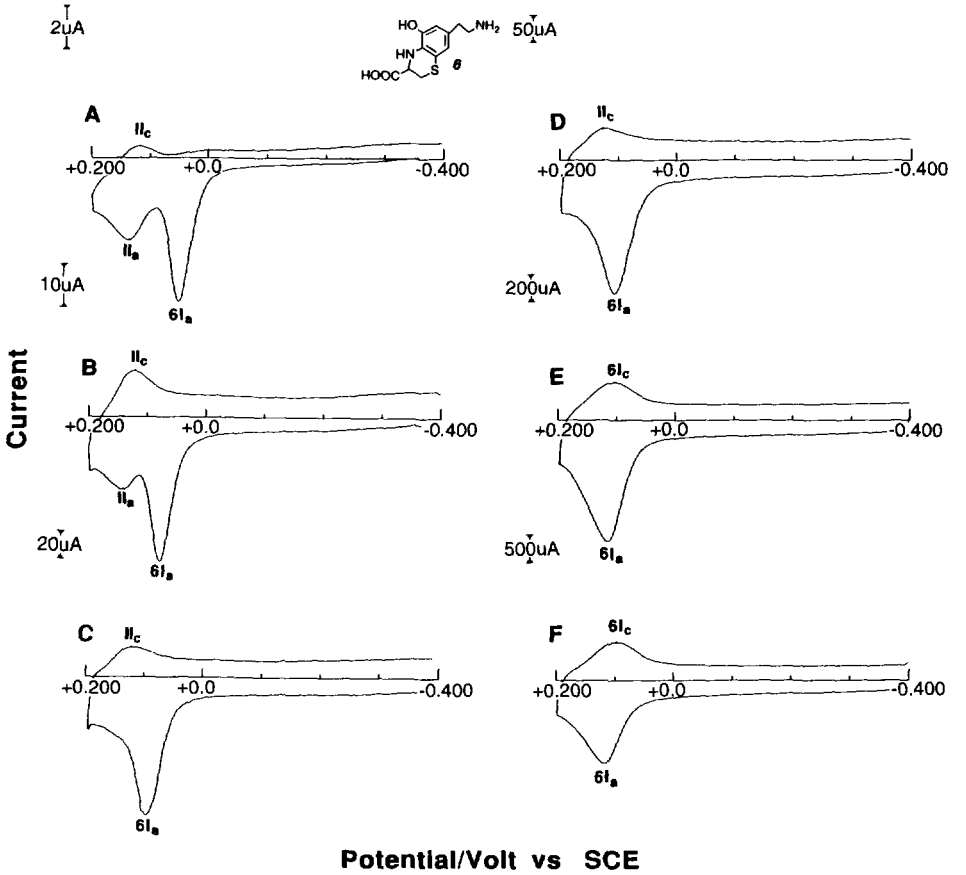

FIG. 2. Cyclic voltammograms at the PGE of dihydrobenzothiazine **6** (1.0 mM) in pH 7.4 phosphate buffer at sweep rates of (A) 10 mVs^{-1}, (B) 100 mVs^{-1}, (C) 500 mVs^{-1}, (D) 1.0 Vs^{-1}, (E) 5 Vs^{-1}, and (F) 10 Vs^{-1}.

and slow reaction. A second more rapid and predominant reaction of cation radical **31** is proposed to be its disproportionation to give **6** and *o*-quinone imine **5**. Thus, this reaction, which occurs as a result of the peak $6I_a$ oxidation of **6**, leads to the product of the peak II_a reaction, i.e., **5**. Accordingly, at intermediate sweep rates (ν = 500 mVs^{-1} – 1 Vs^{-1}; Figs. 2C and 2D) peak II_a does not appear in cyclic voltammograms of **6** but, as a result of disproportionation of **31** to **5** (and **6**) reduction peak II_c still continues to be observed. At sweep rates $\geq$ 5 Vs^{-1} (Figs. 2E and 2F) peak II_c is replaced by reduction peak $6I_c$ at more negative potentials. Under these conditions the disproportionation and deprotonation reactions are outrun so that peak $6I_c$ corresponds to the reversible one-electron reduction of **31** to **6**. The ultimate product of electrochemical oxidation of **6** is benzothiazine **15** formed by rearrangement (tautomerization) of *o*-quinone imine **5**.

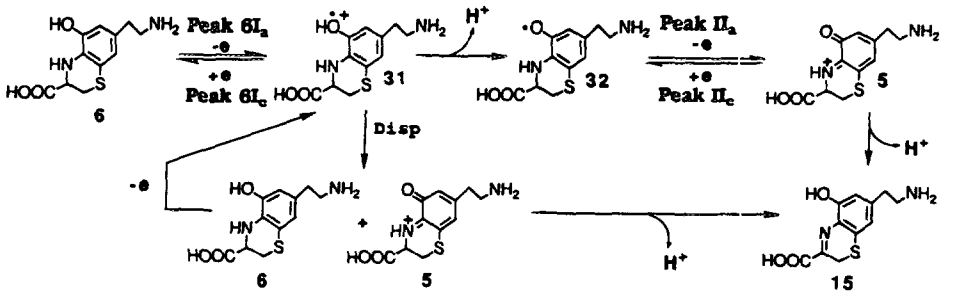

SCHEME III

At pH 7.4 dihydrobenzothiazine **6** and benzothiazine **15** are formed as the initial products of the controlled potential electro-oxidation of 5-*S*-CyS-DA. Information bearing on the oxidation chemistry of 5-*S*-CyS-DA can be deduced from a consideration of the cyclic voltammetry of this compound at pH 7.4 (Fig. 3). On the initial anodic sweep (ν = 100 mVs^{-1}) the primary oxidation peak I_a (E_p = 94 mV) is followed by an indistinct shoulder (oxidation peak II_a, $E_p \approx$ 140–145 mV) and, at more positive potentials, oxidation peak III_a (E_p = 580 mV). After scan reversal reduction peak II_c (E_p = 122 mV) forms a reversible couple with oxidation peak II_a. Peak III_a corresponds to the oxidation of benzothiazine **15** to unknown products. The E_p values of peaks II_a and II_c are identical to those having the same designation in cyclic voltammograms of dihydrobenzothiazine **6** (Fig. 1). Accordingly, it can be

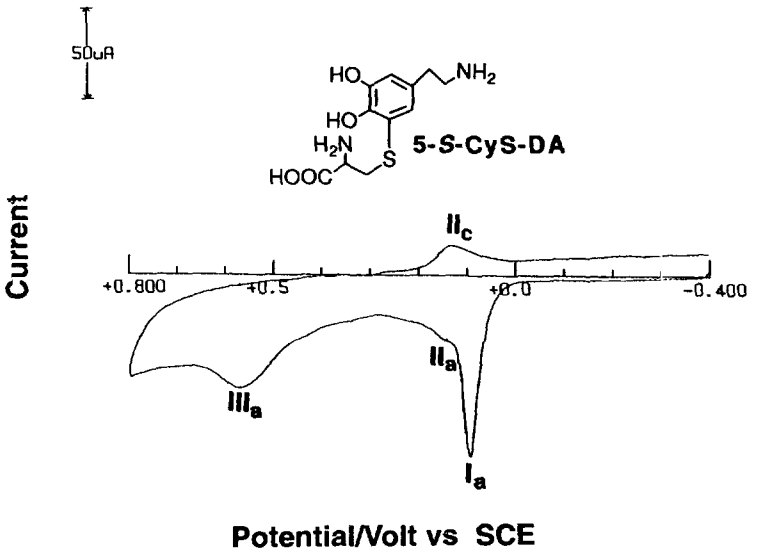

FIG. 3. Cyclic voltammogram at the PGE of 1.0 mM 5-*S*-CyS-DA in pH 7.4 phosphate buffer. Sweep rate, 100 mVs^{-1}.

concluded that the peak I_a oxidation of 5-*S*-CyS-DA, under the conditions employed in Fig. 3, results in formation of trace amounts of radical **32** (peak II_a), *o*-quinone imine **5** (peak II_c), and **15** (peak III_a). A key observation that emerges from the cyclic voltammogram of 5-*S*-CyS-DA (Fig. 3) is that after scanning through oxidation peak I_a (E_p = 94 mV) and the ill-defined peak II_a a significant peak II_c (E_p = 122 mV) corresponding to reduction of *o*-quinone imine **5** appears. The E_p of peak II_c is such that **5** should be capable of chemically oxidizing 5-*S*-CyS-DA. The electrochemical and chemical reactions associated with the various peaks observed in cyclic voltammograms of 5-*S*-CyS-DA are summarized in Scheme IV. Thus, oxidation ($2e$, $2H^+$) of 5-*S*-CyS-DA at peak I_a gives *o*-quinone **4** that very rapidly cyclizes to *o*-quinone imine **5** (*14*). The latter compound then chemically oxidizes 5-*S*-CyS-DA to **4** with concomitant formation of radical **31** that disproportionates to give dihydrobenzothiazine **6** and *o*-quinone imine **5**. Under controlled potential electrolysis conditions **5** would be swept from the electrode surface into the bulk solution where it reacts with 5-*S*-CyS-DA to give **6** and **5** and hence **15** such that **6** and **15** are detectable products in the early stages of the reaction. With more prolonged electrolysis **6** is further oxidized to **15** by the reactions shown in Scheme III. Further insights into the oxidation chemistry of 5-*S*-CyS-DA can be drawn from the cyclic voltammograms presented in Fig. 4. At a very slow sweep rate (10 mVs^{-1}, Fig. 4A) peak I_a (E_p = 69 mV) corresponds to the oxidation of 5-*S*-CyS-DA via **4** to *o*-quinone imine **5**. Chemical oxidation of 5-*S*-CyS-DA by **5** (to **4**) then yields radical **31**. At slow sweep rates partial deprotonation of **31** yields radical **32** which is then oxidized at peak II_a to **5**. At such slow sweep rates rearrangement of **5** to **15** must be extensive with the result that very little of the former compound remains at the electrode surface and, hence, reduction peak II_c is virtually absent on the reverse cycle. With increasing sweep rates i_p for oxidation peak II_a decreases relative to that for peak I_a (Figs. 4B and 4C) and ultimately this peak disappears (ν = 200 mVs^{-1}; Fig. 4D). The decrease of i_p for peak II_a with increasing sweep rate thus reflects the relatively slow deprotonation of **31** to **32**. The fact that peak II_c remains over the same sweep rate range is, therefore, indicative of the faster rate of disproportionation of **31** to **5** (and **6**). Similar reaction pathways occur as a result of the electrochemical oxidation of **9** leading, initially, to dihydrobenzothiazine **16** and benzothiazine **17**. Controlled potential electro-oxidation of **9** ultimately yields **17** as a result of oxidation of **16**.

DISCUSSION

Presently available information indicates that the black insoluble indolic neuromelanin that normally pigments dopaminergic cell bodies in the SN is formed as a consequence of autoxidation of DA (*8, 9*) in the absence of GSH or CySH (*10*). In the event that the resulting DA-*o*-quinone is not reduced to DA by cytoplasmic antioxidants, particularly ascorbic acid, then it must cyclize to 5,6-dihydroxyindoline (**1**; Scheme I). Once this initial cyclization has occurred then ultimate formation of neuromelanin is probably inevitable. This is so because the known key intermediates formed in the early stages of the melanin pathway, i.e., **1** and 5,6-DHI, are more

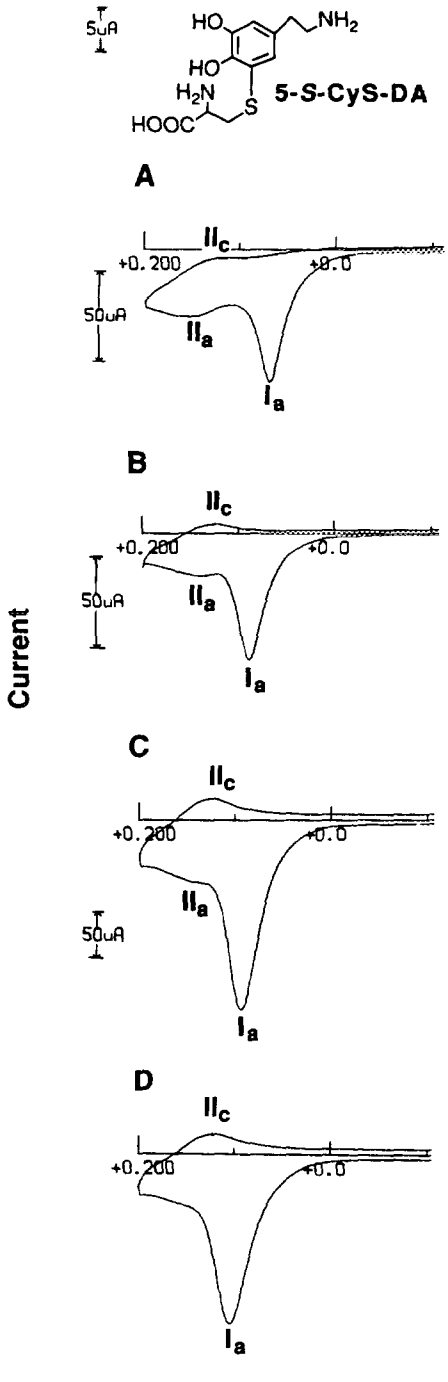

FIG. 4. Cyclic voltammograms at the PGE of 5-*S*-CyS-DA (1.0 mM) in pH 7.4 phosphate buffer at sweep rates of (A) 10 mVs^{-1}, (B) 50 mVs^{-1}, (C) 100 mVs^{-1}, and (D) 200 mVs^{-1}.

easily oxidized than DA. The SN neurons most vulnerable to degeneration in PD appear to be those most heavily pigmented with neuromelanin (*27, 28*). These are the neurons which must sustain the highest basal levels of DA autoxidation. For reasons discussed earlier, we have proposed that a key step in the pathogenesis of PD might involve an upregulation of nigral γ-glutamyltranspeptidase resulting in the translocation of GSH and/or CySH into the cytoplasm of dopaminergic SN cells (*14*). This would be expected to divert the neuromelanin pathway as a result of GSH/CySH scavenging DA-*o*-quinone to give directly or indirectly 5-*S*-CyS-DA as conceptualized in Scheme I (*14*) with, over the course of time, depigmentation of SN neurons and the irreversible loss of GSH without a corresponding increase in GSSG. The voltammetric E_p values (ν = 10 mVs^{-1}) for oxidation of DA and 5-*S*-CyS-DA at pH 7.4 are 133 and 69 mV, respectively (*11, 14*). Based on such data, therefore, the GSH/CySH-mediated diversion of the neuromelanin pathway would give an initial product, 5-*S*-CyS-DA, that is more easily exidized than DA from which it is derived. Thus, in neuromelanin-pigmented SN neurons, where DA is autoxidized, 5-*S*-CyS-DA must also be oxidized. However, an unusual aspect of this oxidation reaction, at least under electrochemical conditions, is that the facile intramolecular cyclization of *o*-quinone **4** leads directly to bicyclic *o*-quinone imine **5**. The latter compound, based on both its redox potential and the results of this investigation, is capable of chemically oxidizing 5-*S*-CyS-DA. Thus, the *in vivo* autoxidation of 5-*S*-CyS-DA would be expected to yield a product, **5**, that can not only contribute to chemical oxidation of the conjugate but also forms dihydrobenzothiazine **6** (Scheme IV), a compound known to be lethal in the mouse brain (*14*). In principal, once the oxidation of 5-*S*-CyS-DA is initiated to form *o*-quinone imine **5** the oxidation reaction should become self-sustaining to form dihydrobenzothiazine **6**. This does not happen, however, because **5** escapes from the catalytic cycle as a consequence of its rearrangement to benzothiazine **15**. Nevertheless, **5** clearly contributes to the very facile oxidation of 5-*S*-CyS-DA. Dihydrobenzothiazine **6** (E_p = 53 mV at pH 7.4; ν = 10 mVs^{-1}) is an even more easily oxidized compound than DA and 5-*S*-CyS-DA. Accordingly, if the general features of the electrochemically driven oxidation of 5-*S*-CyS-DA (Scheme IV) are also mediated by molecular oxygen in the cytoplasm of dopaminergic SN cells then **6** would be expected to be autoxidized to benzothiazine **15** (Scheme III). The overall result of an influx of GSH and/or CySH into heavily pigmented SN neurons, thus, would be predicted to lead not only to their depigmentation but also to the formation of **6** and **15** and more structurally complex dihydrobenzothiazines and benzothiazines (*14*) that we have suggested might include the endotoxins responsible for the degeneration of nigrostriatal dopaminergic neurons and PD. Indeed, the predicted ease of autoxidation of 5-*S*-CyS-DA and **6** and, perhaps, redox cycling of these compounds in the presence of cytoplasmic antioxidants and molecular oxygen might account for greatly elevated fluxes of reduced oxygen species ($O_{2\cdot-}$, H_2O_2, $HO\cdot$) that contribute to both elevated rates of DA oxidation (*31*) and oxidative stress (*3–5*) that are known to occur in the Parkinsonian SN. Furthermore, it is conceivable that **6, 15,** and related metabolites resulting from the GSH/GySH-mediated diversion of the neuromelanin pathway (*14*) might also contribute to mitochondrial abnormalities in the Parkinsonian SN (*6, 7*).

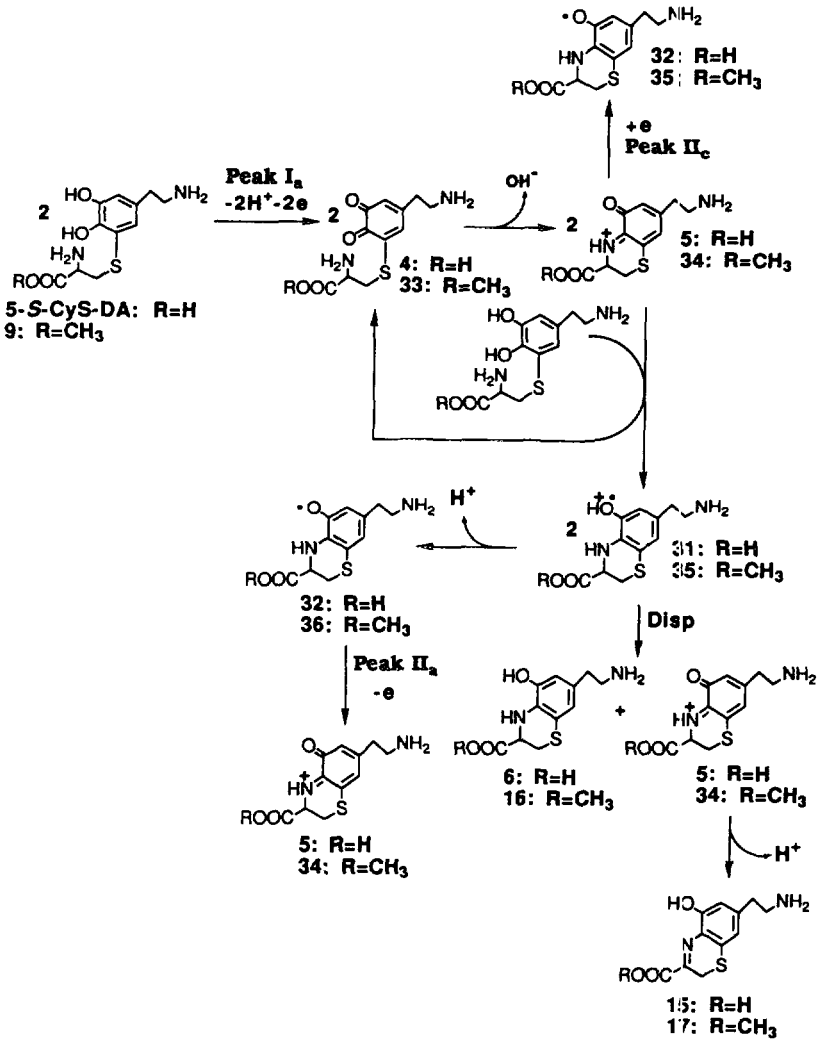

SCHEME IV

Fornstedt *et al.* (*31*) have reported representative levels of DA in human pigmented, depigmented, and Parkinsonian SN tissue to be 2560 ± 456, 939 ± 361, and 231 pmol/g, respectively. This decline in DA levels reflects increasing degeneration of dopaminergic SN neurons in these three patient groups. In the same patient populations the 5-*S*-CyS-DA/DA concentration ratios increased from 0.0254 ± 0.006 to 0.066 ± 0.03 to 0.174, respectively. These results were interpreted to indicate an increase in the rate of autoxidation of DA with increasing depigmentation and degeneration of SN neurons. This interpretation is based on the premise that 5-*S*-CyS-DA is a marker molecule for intraneuronal DA autoxidation. However, the

results of this and an earlier study (*14*) suggest that 5-*S*-CyS-DA levels would in fact be a rather poor indicator of DA autoxidation rates because of the fact that this conjugate is more easily oxidized than the neurotransmitter and because of the catalytic role of *o*-quinone imine **5** in its oxidation chemistry (Scheme IV). Support for this view is provided by the observations that the absolute concentrations of 5-*S*-CyS-DA measured in pigmented, depigmenting, and Parkinsonian SN tissue were not only very low but were virtually identical (*31*). The results of the present *in vitro* study suggest that benzothiazine **15**, the final product of oxidation of 5-*S*-CyS-DA and dihydrobenzothiazine **6**, might represent both a better marker molecule for intraneuronal oxidation of DA and a role for GSH/CySH in the neurodegenerative processes that occur in PD. Under the conditions employed in the current *in vitro* investigation **15** was relatively stable in solution at physiological pH. However, attempts to isolate this compound or its methyl ester **17** in the solid state were unsuccessful owing to their transformation to a number of unidentified secondary products. The fact that the 2,2-dimethyl-substituted benzothiazines **13** and **14** could be isolated implies that the unsubstituted C(2)-position in **15** (and **17**) is a reactive center. Indeed, it has been proposed that related benzothiazines thought to be formed upon oxidation of 5-*S*-CyS-DOPA undergo spontaneous dimerization at the C(2)-position to give trichochromes, precursors of pheomelanin polymers (*45, 46*).

ACKNOWLEDGMENTS

This work was supported by the National Institutes of Health Grant No. NS-29886 and by funds provided by the PI Research Investment Program, the Vice President for Research and Research Council at the University of Oklahoma. The authors thank Dr. X-M Shen for performing some cyclic voltammetry experiments.

REFERENCES

1. Hornykiewicz, O., and Kish, S. J. (1986) *Adv. Neurol.* **45,** 19.
2. Hornykiewicz, O. (1989) *Prog. Neuropsychopharmacol. Biol. Psychiatry* **13,** 319.
3. Dexter, D. T., Carter, C. J., Wells, F. R., Javoy-Agid, F., Lees, A. J., Jenner, P., and Marsden, D. C. (1989) *J. Neurochem.* **52,** 381.
4. Jenner, P., Schapira, A. H. V., and Marsden, D. C. (1992) *Neurology* **42,** 2241.
5. McGeer, P. L., Itagaki, S., Akiyama, H., and McGeer, E. G. (1989) *in* Parkinsonism and Aging (Calne, D. B., Comi, G. Crippa, A., Horowski, R., and Trabucchi, M., Eds.), pp. 25–34, Raven Press, New York.
6. Schapira, A. H. V., Cooper, J. M., Dexter, D., Jenner, P., Clark, J., and Marsden, D. C. (1990) *Lancet* 1269.
7. Schapira, A. H. V., Cooper, J. M., Dexter, D., Clarke, J. B., Jenner, P., and Marsden, D. C. (1990) *J. Neurochem.* **54,** 823.
8. Graham, D. G. (1978) *Mol. Pharmacol.* **14,** 633.
9. Rodgers, A. D., and Curzon, G. (1975) *J. Neurochem.* **24,** 1123.
10. Carstam, R., Brinck, C., Hindemith-Augustsson, A., Rorsman, H., and Rosengren, E. (1991) *Biochim. Biophys. Acta* **1097,** 152.
11. Zhang, F., and Dryhurst, G. (1993) *Bioorg. Chem.* **21,** 392.
12. Tse, D. C., McCreery, R. L., and Adams, R. N. (1976) *J. Med. Chem.* **19,** 37.

13. YOUNG, T. E., AND BABBITT, B. W. (1983) *J. Org. Chem.* **48,** 562.
14. ZHANG, F., AND DRYHURST, G. (1994) *J. Med. Chem.* **37,** 1084.
15. SLIVKA, A., MYTILINEOU, C., AND COHEN, G. (1987) *Brain Res.* **409,** 275.
16. PHILBERT, M. A., BEISWANGER, C. M., WATERS, D. K., REUHL, K. R., AND LOWNDES, H. E. (1990) *Toxicol. Appl. Pharmacol.* **107,** 215.
17. PERRY, T. L., GODIN, D. A., AND HANSON, S. (1982) *Neurosci. Lett.* **33,** 305.
18. FARIELLO, R. G., CALABRESE, V., AND NAPPI, G. (1988) *in* Neurodegenerative Disorders: The Role of Endotoxins and Xenobiotics (Nappi, G., Ed.), pp. 81–92, Raven Press, New York.
19. FARIELLO, R. G., GHILARDI, O., PESCHECHERA, A., RAMUCCI, M. T., AND ANGELUCCI, T. (1988) *Neuropharmacology* **27,** 1077.
20. CALABRESE, V., AND FARIELLO, R. G. (1988) *Biochem. Pharmacol.* **37,** 2287.
21. HALLIWELL, B., AND GUTTERIDGE, M. C. (1984) *Biochem. J.* **219,** 1.
22. WALLING, C. (1975) *Acc. Chem. Res.* **8,** 125.
23. COHEN, G. (1983) *J. Neural Transm.* **19,** 89.
24. AMBANI, L. M., MELVIN, H., VAN WOERT, M. H., AND MURPHY, S. (1975) *Arch. Neurol.* **32,** 114.
25. MCGEER, P. L., MCGEER, E. G., AND SUZUKI, J. S. (1976) *Arch. Neurol.* **34,** 33.
26. MANN, D. M. A. (1983) *Mech. Ageing Dev.* **21,** 193.
27. KASTNER, A., HIRSCH, E. C., LEJEUNE, O., JAVOY-AGID, F., ROSCOL, O., AND AGID, Y. (1992) *J. Neurochem.* **59,** 1080.
28. HIRSCH, E. C., GRAYBIEL, A. M., AND AGID, Y. (1988) *Nature* **334,** 345.
29. ROSENGREN, E., LINDER-ELIASSON, E., AND CARLSSON, A. (1985) *J. Neural Transm.* **63,** 247.
30. FORNSTEDT, B., ROSENGREN, E., AND CARLSSON, A. (1986) *Neurophamacology* **25,** 451.
31. FORNSTEDT, B., BRUN, A., ROSENGREN E., AND CARLSSON, A. (1989) *J. Neural Transm.* [P-D Sect.] **1,** 279.
32. SIAN, J., DEXTER, D. T. JENNER, P., AND MARSDEN, D. C. (1992) *Br. J. Pharmacol.* **107** (Suppl.), 428P.
33. MEISTER, A. (1974) *Life Sci.* **15,** 177.
34. JENNER, P., DEXTER, D. T., SIAN J., SCHAPIRA, A. H. V., AND MARSDEN, D. C. (1992) *Ann. Neurol.* **32** (Suppl.), S82.
35. REIDERER, P., SOFIC, E., RAUSCH, W. D., SCHMIDT, B., REYNOLDS, G. P., JELLINGER, K., AND YOUDIM, M. B. H. (1989) *J. Neurochem.* **52,** 515.
36. GIBB, W. R. G., AND LEES, A. J. (1988) *J. Neurol. Neurosurg. Psychiatry* **51**, 757.
37. KISH, S. J., MORITO, C., AND HORNYKIEWICZ, O. *Neurosci. Lett.* **58,** 343.
38. PERRY, T. L., AND YONG, V. (1986) *Neurosci. Lett.* **67,** 269.
39. RAPS, S. P., LAI, J. C. K., HERTZ, L., AND COOPER, A. J. L. (1989) *Brain Res.* **493,** 398.
40. SAGARA, J. I., MIURA, K., AND BANNAI, S. (1993) *J. Neurochem.* **61,** 1672.
41. OWENS, J. L., MARSH, H. A., AND DRYHURST, G. (1978) *J. Electroanal. Chem. Interfacial Electrochem.* **91,** 231.
42. ITO, S., AND PROTA, G. (1977) *Experientia* **33,** 1118.
43. STERNSON, A. W., MCCREERY, R., FEINBERG, B., AND ADAMS, R. N. *J. Electroanal. Chem. Interfacial Electrochem.* **46,** 313.
44. DRYHURST, G., KADISH, K. M., SCHELLER, F., AND RENNEBERG, R. (1982) Biological Electrochemistry, Vol. I, pp. 1–111, Academic Press, New York.
45. CHEDEKEL, M. R., SUBBARAO, K. V., BHAN, P., AND SCHULTZ, T. M. (1987) *Biochim. Biophys. Acta* **912,** 239.
46. CRIPPA, R., HORAK, V., PROTA, G., SVORNOS, P., AND WOLFROM, L. (1989) *Alkaloids* **36,** 253.